

A new method for classification and characterization of voltage sags

Mladen Kezunovic *, Yuan Liao

Department of Electrical Engineering, Texas A&M University, College Station, TX 77843-3128, USA

Accepted 8 March 2001

Abstract

This paper presents new software developments related to sag classification and characterization. A new fuzzy rule based algorithm for classifying the types of voltage sags is proposed. The voltage sags are categorized into three types, i.e. sags due to the faults, large motor starting, or due to interaction between motor operation and faults. Three distinctive features of sag waveforms are defined and extracted first. Then a fuzzy logic based inference engine utilizing these features as inputs is implemented for decision making. Also presented are the characterization methods and suggested monitoring parameters for each of the three types of sags. Finally the application of the proposed characterization approaches for the equipment sensitivity study is illustrated. The results of case studies are reported. The presented approach has been implemented in MATLAB. © 2001 Elsevier Science B.V. All rights reserved.

Keywords: Voltage sag; Fuzzy logic; Pattern classification; Parameter estimation; Power quality

1. Introduction

Among various types of power quality disturbances in a power system, voltage sags are particularly troublesome since they occur rather randomly and their characteristics are difficult to predict. More importantly, voltage sags may cause trips or mis-operations of industrial equipment. The increased use of sensitive electronic control circuitry has made modern equipment far more vulnerable to voltage sag events than ever [1,2].

As known, the trip or mis-operation of modern equipment can not just be attributed to the sag magnitude and duration any more. Instead, other factors like point-on-wave, unbalance ratio, and phase angle shift may also play an essential role in the behavior of the modern loads during voltage sag events. In order to improve the immunity or ride-through ability of the equipment to the sag events and thus enhance the coordination between the system and the equipment, a good appreciation of how various sag parameters affect the equipment operating characteristics is very helpful [2–4].

Serving such purposes, IEEE P1159.2 has initiated a project on the sag characterization based on digitally sampled data. So far, this task force has proposed a draft on the characterization of sags caused by the faults. It is known that the sags may be caused by large motor starting as well. In addition, the interaction between the motor operation and the faults has also a significant effect on the voltage sag characteristics [5,6]. Therefore, to accurately characterize these different types of sags, pertinent parameters need to be defined for each of these three types of sags. This paper contributes to this aspect.

In order to select appropriate algorithms for characterization, the voltage sag waveforms need to be classified first. Manual classification is tedious, time consuming and sometimes even difficult. Therefore, this paper proposes a new fuzzy logic based system for automatic sag classification.

In the rest of the paper, the fuzzy logic based sag classifier is described first. Then the proposed characterization approaches for the three types of sag events are described. Next, the equipment sensitivity study utilizing the characterization results is illustrated. Case studies and results for the characterization and equipment characteristic evaluation studies are reported.

* Corresponding author.

E-mail address: kezunov@ee.tamu.edu (M. Kezunovic).

2. The proposed sag classification algorithm

This section presents a fuzzy rule based classification system for identifying the types of the sags. It is assumed that the input waveforms have already been detected as voltage sag events by another general classification system [2]. The method presented here further classifies the sag events into fault related sags (FRS), large motor starting related sags (MSRS), or motor re-acceleration related sags (MRRS). The MRRS are caused by the interaction between the fault and large motor operation. The proposed classification system consists of the feature extraction phase and the decision making phase as illustrated in Sections 2.1 and 2.2, respectively.

2.1. Feature extraction

To demonstrate how distinctive features for each type of voltage sags can be extracted, a number of sag waveforms of various types have been obtained using Electromagnetic Transients Program (EMTP). Figs. 1–3 show the typical waveforms for each of the three types of sags and the related rms plots obtained by applying the Fourier transform.

The simulation sensitivity studies have shown that each type of the sags has distinct characteristics. For the FRS, the initial drop and the final recovery of the sag are very quick. For the MSRS, the recovery of the sag takes a long time, normally ranging from several hundred milliseconds to several seconds. For the MRRS, at the beginning of the fault, the large motor acts as a voltage source and thus reduces the voltage drop. After the fault is cleared, the re-acceleration of the motor deepens the sag and thus prolongs the recovery of the voltage sag [6]. In addition, the fault related sags normally result in a relatively larger phase angle shift than the non-fault related sags.

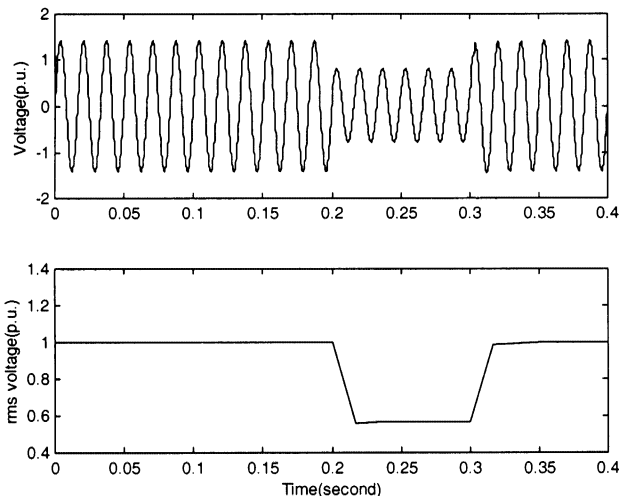


Fig. 1. A fault related voltage sag signal and its rms plot.

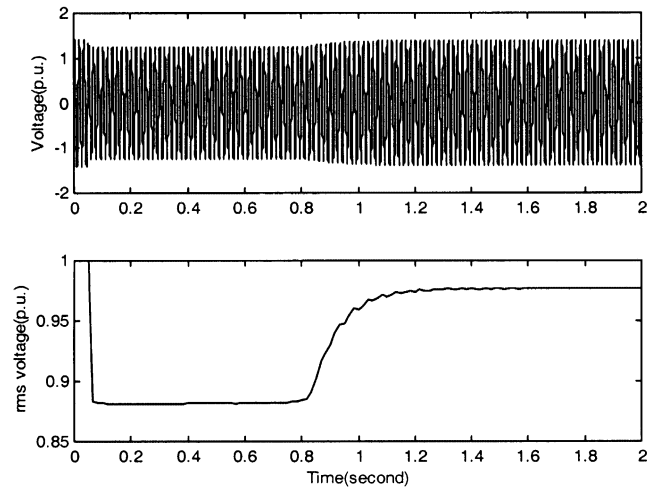


Fig. 2. A motor starting related voltage sag signal and its rms plot.

Based on the above analysis, the following three features have been extracted and will be used as inputs to the decision-making system.

1. Initial phase angle shift (α_{pasi}): This is defined as the difference between the phase angle of the during-sag waveform and that of the reference waveform. The reference waveform is defined as the pre-sag normal steady state waveform.
2. Recovery period (RP): This is defined as the duration entailed for the voltage magnitude to recover to its normal value. The recovery period is expressed in cycles of the fundamental frequency.
3. Voltage change (VC): This is defined as the difference between the voltage magnitude at the initial recovery time and the voltage magnitude one cycle later.

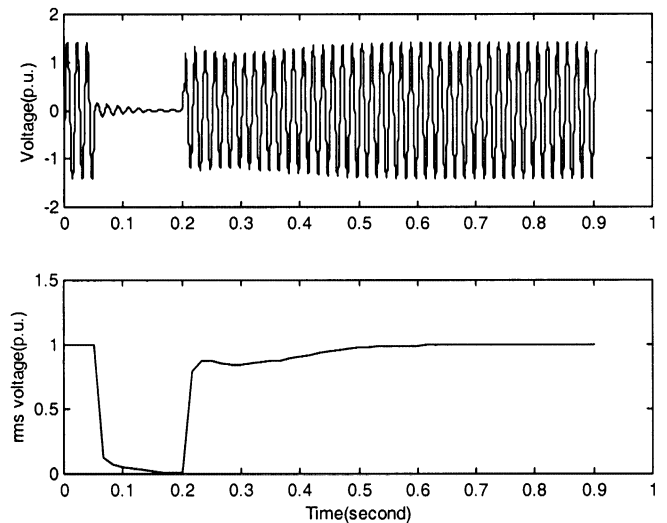


Fig. 3. A voltage sag signal caused by the fault and motor re-acceleration and its rms plot.

These parameters are obtained using the following equations. The nomenclature is listed at the end of the paper.

$$\alpha_{\text{pasi}} = 180[\text{angle}(V^s[1]) - \text{angle}(V^1[1])]/\pi \quad (1)$$

where, $V^n[k]$ is the Discrete Fourier Transform (DFT) for the samples contained in the n th data window defined as

$$V^n[k] = \sum_{i=0}^{N-1} v[i + (n-1)N]e^{-j2\pi ki/N}, \quad n = 1, 2, \dots, \text{round}(L/N) \quad (2)$$

$v[i]$: the sampled signal, $i = 0, 1, \dots, L-1$, with L the length of the signal.

$$i_s = \text{index_s}\{\text{abs}(WC_1[k]) - \varepsilon\}/L_{wc_1}L \quad (3)$$

$$V^s[k] = \sum_{i=i_s}^{i_s+N-1} v[i]e^{-j(2\pi ki/N)} \quad (4)$$

$$V_{\text{rms}}[n] = \sqrt{\frac{1}{N} \sum_{i=0}^{N-1} v^2[i + (n-1)N]} \quad (5)$$

V_{rms}^t is defined as an array composed of $V_{\text{rms}}[n]$, $n = 1, 2, \dots, L_{\text{rms}}^t$ with $L_{\text{rms}}^t = \text{round}(L/N)$.

$$V_{\text{min}} = \min(V_{\text{rms}}^t) \quad (6)$$

$$i_{\text{min}} = \text{index_min}(V_{\text{rms}}^t) \quad (7)$$

$V_{\text{rms}}^{\text{td}}$ is defined as an array composed of $V_{\text{rms}}[n]$, $n = i_{\text{min}}, \dots, L_{\text{rms}}^t$

$$i_{\text{re}} = \text{index_s}(V_{\text{rms}}^{\text{td}} - 1.05V_{\text{min}}) \quad (8)$$

$$V_{\text{fin}} = V_{\text{rms}}[L_{\text{rms}}^t] \quad (9)$$

$$i_{\text{ec}} = \text{index_s}(V_{\text{rms}}^{\text{td}} - 0.96V_{\text{fin}}) \quad (10)$$

Then, we obtain

$$RP = i_{\text{ec}} - i_{\text{re}} \quad (11)$$

$$VC = v_{\text{rms}}^{\text{td}}[i_{\text{re}} + 1] - v_{\text{rms}}^{\text{td}}[i_{\text{re}}] \quad (12)$$

$WC_1[k]$ is the first scale wavelet detail coefficients, $k = 1, 2, \dots, L_{WC_1}$, with L_{WC_1} the length of the detail coefficients. Daubechies-4 wavelet family is used in our work [2]. It is shown that the type of the wavelet does not have a significant impact on the results because different type of wavelets differs in the regularity, symmetry or compactness of support, etc. However, we mainly utilize the time localization characteristics of the wavelet for accurately obtaining the time parameters of the events. The wavelet families of Daubechies wavelet, Morlet wavelet, symlets, coiflets and biorthogonal spline wavelets have been demonstrated to work similarly well for the applications presented here.

ε is a pre-defined constant, selected as 0.05 here.

$\text{angle}(\cdot)$ gives the angle of the argument in radians.

$\text{index_s}(\cdot)$ yields the index of the first element that is greater than zero of the input array.

$\text{index_min}(\cdot)$ gives the index of the minimum value of the argument.

$\text{round}(\cdot)$ gives the integer part of the argument.

$\text{min}(\cdot)$ gives the minimum value of the argument.

Eqs. (1), (11) and (12) give features for each single phase signal. If the input voltages include three-phase signals, then the features for each phase are obtained, and the largest value of the three phases is selected as the extracted feature.

2.2. The proposed sag classification algorithm

The rule sets of the fuzzy rule based system are presented as follows.

1. If RP is b_2 and α_{pasi} is a_1 , then $\text{MSRS} = 1$;
2. If RP is b_2 and α_{pasi} is a_2 and VC is c_2 then $\text{MRRS} = 1$;
3. If RP is b_2 and α_{pasi} is a_2 and VC is c_1 then $\text{MSRS} = 1$;
4. If RP is b_1 then $\text{FRS} = 1$;

In the above rules, a_i , b_i and c_i are the membership functions for the input features, and the following trapezoidal functions are used to describe them. Detailed description of this function is referred to [7].

$$\mu(x) = \text{trapmf}(a, b, c, d)$$

$$= \begin{cases} (x-a)/(b-a) & a \leq x \leq b \\ 1 & b \leq x \leq c \\ (x-d)/(c-d) & c \leq x \leq d \\ 0 & \text{otherwise} \end{cases} \quad (13)$$

The fuzzy partitions and the according membership functions can be obtained based on both the statistical studies and the expert's knowledge. Opinions from operators can be conveniently incorporated into the system in practical applications [7]. The membership functions for the features are shown as follows.

Initial phase angle shift ($^\circ$):

$$a_1: \text{trapmf}(-0.18, -0.02, 4, 4.5)$$

$$a_2: \text{trapmf}(4, 4.5, 361, 362)$$

Recovery period (cycles)

$$b_1: \text{trapmf}(-0.18, -0.02, 2, 4)$$

$$b_2: \text{trapmf}(1, 3, 1000, 1001)$$

Voltage change (p.u.)

$$c_1: \text{trapmf}(-0.18, -0.02, 0.04, 0.05)$$

$$c_2: \text{trapmf}(0.04, 0.05, 1.1, 1.2)$$

The outputs of the classification system are the variables 'FRS', 'MSRS' and 'MRRS' whose values represent the degree to which the event belongs to each of these categories. The type of the event will be selected based on the largest membership value. In cases where two or more types of sags have the same largest membership value, all of them will be subjected to further analysis.

2.3. Evaluation studies

A number of sag events of the concerned types have been generated by EMTP, and then the proposed algorithm is applied for classification of these events. The correct identification rate of the system is about 99%. In most of the mis-classified cases, the motor starting related sags are mistakenly classified as fault related sags. This is because in these cases the recovery time of the motor starting may be too short for identification.

3. The proposed approaches for characterizing sag events

Once the type of the sag events is identified, they can be further characterized using the approaches described in this section. In the following discussions, the voltage is in p.u., time in seconds, and angle in degrees unless specially specified.

3.1. Characterization of FRS

The parameters for characterizing FRS include the minimum rms value V_{\min} , maximum rms value V_{\max} , average rms value V_{ave} , final rms value V_{fin} , peak value V_p , sag starting time t_s , sag end time t_e , sag duration t_{sd} , initialization angle α_{ini} , initial phase angle shift α_{pasi} , initial phase angle shift rate r_{pasi} , end angle α_{end} , end phase angle shift α_{pase} , end phase angle shift rate r_{pase} , total harmonic distortion THD, rms magnitude unbalance ratio r_{ub} , and three-phase phase angle difference deviation PADD [2,3]. α_{pasi} , V_{\min} and V_{fin} are given by Eqs. (1), (6) and (9), respectively. The other parameters are obtained as follows.

$$V_{\max} = \max(V_{\text{rms}}^t) \quad (14)$$

$$V_{\text{ave}} = \text{ave}(V_{\text{rms}}^t) \quad (15)$$

$$i_p = \text{index_max}\{\text{abs}(v[i])\} \quad (16)$$

$$V_p = v[i_p] \quad (17)$$

$$t_s = i_s/f_s \quad (18)$$

$$i_e = \text{index_e}\{\text{abs}(WC_1[k]) - \varepsilon\}/L_{wc}L \quad (19)$$

$$t_e = i_e/f_s \quad (20)$$

$$t_{\text{sd}} = t_e - t_s \quad (21)$$

$$i_{-z} = \text{index_z}(v[i], i_s) \quad (22)$$

$$\alpha_{\text{ini}} = 360(i_s - i_{-z})f_0/f_s \quad (23)$$

$$r_{\text{pasi}} = \alpha_{\text{pasi}} f_0 \quad (24)$$

$$i_{ze} = \text{index_z}(v[i], i_e) \quad (25)$$

$$\alpha_{\text{end}} = 360(i_e - i_{ze})f_0/f_s \quad (26)$$

$$\alpha_{\text{pase}} = 180[\text{angle}(V^s[1]) - \text{angle}(V^s[1])]/\pi \quad (27)$$

$$r_{\text{pase}} = \alpha_{\text{pase}} f_0 \quad (28)$$

$$\text{THD} = \sqrt{\frac{\text{round}(N/2)}{\sum_{k=2}^{\text{round}(N/2)} \text{abs}(V^s[k])^2}} \quad (29)$$

$$r_{\text{ub}} = [\max(V_{\text{rmsabc}}) - \min(V_{\text{rmsabc}})]/\text{ave}(V_{\text{rmsabc}}) \quad (30)$$

$$\text{PADD} = 180\max\{\text{abs}(P_{\text{pad}})\}/\pi \quad (31)$$

In the above equations, we have defined

$$V_{\text{rms}} = \sqrt{\frac{1}{N} \sum_{i=0}^{N-1} v^2[i + i_s]} \quad (32)$$

V_{rmsabc} is defined as the array composed of V_{rmsa} , V_{rmsb} , and V_{rmsc} that are obtained by applying Eq. (32) to phase a, b and c voltage signal, respectively.

$$V^e[k] = \sum_{i=i_e}^{i_e+N-1} v[i] e^{-j(2\pi k i/N)} \quad (33)$$

$$P_{\text{ab}} = \text{angle}(V^{\text{sa}}[1]) - \text{angle}(V^{\text{sb}}[1]) \quad (34)$$

$$P_{\text{bc}} = \text{angle}(V^{\text{sb}}[1]) - \text{angle}(V^{\text{sc}}[1]) \quad (35)$$

$$P_{\text{ca}} = \text{angle}(V^{\text{sc}}[1]) - \text{angle}(V^{\text{sa}}[1]) \quad (36)$$

V^{sa} , V^{sb} and V^{sc} are obtained by applying Eq. (4) to phase a, b and c signal respectively.

$$P_{\text{pad}} = [P_{\text{ab}} - 2\pi/3, P_{\text{bc}} - 2\pi/3, P_{\text{ca}} - 2\pi/3] \quad (37)$$

$\text{abs}(\cdot)$ gives the absolute value of the argument
 $\text{index_e}(\cdot)$ yields the index of the last element that is greater than zero of the input array
 $\text{index_max}(\cdot)$ gives the index of the maximum value of the argument
 $\text{index_z}(\cdot, \cdot)$ gives the index of the positive zero crossing point of the first array argument that is closest to and prior to the second scalar argument
 $\text{max}(\cdot)$ gives the maximum value of the argument
 $\text{ave}(\cdot)$ gives the mean of the argument

3.2. Characterization of MSRS

Compared to the characterization of FRS, characterization of MSRS entails two new parameters, i.e. sag recovery time t_{re} and recovery duration t_{rd} . On the other hand, the end angle, end angle shift and end angle shift rate are eliminated because the MSRS voltage recovers very slowly and it is hard to accurately define and compute these three parameters. It is also found that wavelet transform can accurately locate the starting and end time of FRS, but usually fails to do so for MSRS. Hence, the following different approaches for characterizing MSRS are described.

Fig. 4 depicts the rms plot of a typical MSRS signal for illustrating the definitions of some parameters. In the figure, t_{re} is the sag recovery time and t_e is the end time of the sag. t_{re} and t_e can be computed as follows.

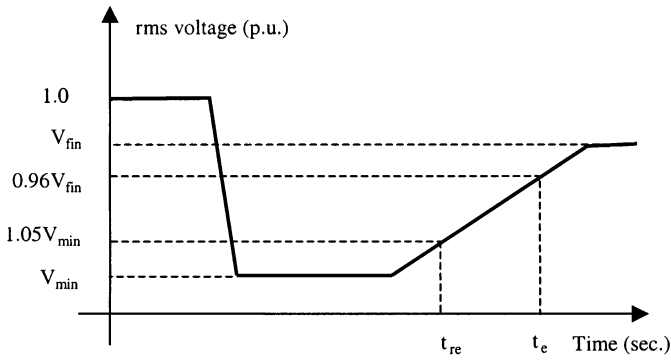


Fig. 4. Illustration of MSRS parameters.

$$t_{re} = (i_{re} + i_{min} - 1)/f_0 \quad (38)$$

$$t_e = (i_{ec} + i_{min} - 1)/f_0 \quad (39)$$

$$t_{rd} = t_{re} - t_s \quad (40)$$

$$t_{sd} = t_e - t_s \quad (41)$$

i_{min} , i_{re} and i_{ec} are referred to Eqs. (7), (8) and (10), respectively.

Parameters V_{min} , V_{max} , V_{ave} , V_{fin} , V_p , t_s , α_{ini} , α_{pasi} , r_{pasi} , THD, r_{ub} and PADD are calculated in the same way as FRS.

3.3. Characterization of MRRS

Compared to MSRS, one new parameter, the initial rms value V_{ini} is added. This reflects the fact that the motor in MRRS acts as a voltage source at the beginning of the fault, and thus the voltage gradually reduces to the lowest magnitude rather than suddenly reducing to the lowest value as in FRS or MSRS. All the other parameters are the same as those for MSRS except that the recovery time t_{re} is calculated in a different way. Fig. 5 shows the rms plot of a typical MRRS voltage signal. V_{ini} and t_{re} are obtained as follows.

$$V_{ini} = V_{rmss} \quad (42)$$

$$t_{re} = i_{min}/f_0 \quad (43)$$

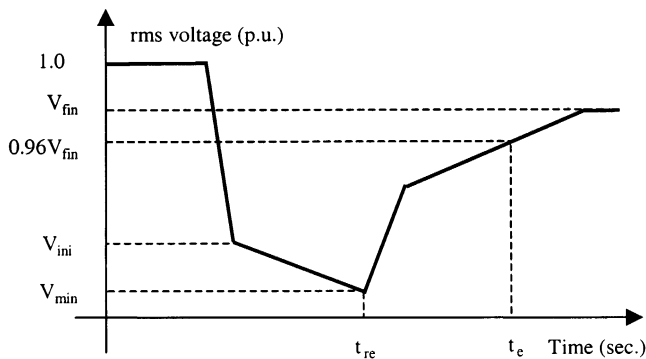


Fig. 5. Illustration of MRRS parameters.

Table 1
Parameters for the sag shown in Fig. 1

Sag parameters	Values
Minimum rms value (p.u.)	0.56
Maximum rms value (p.u.)	1.0
Average rms value (p.u.)	0.89
Final rms value (p.u.)	1.0
Peak value (p.u.)	1.45
Sag starting time (ms)	199.83
Sag end time (ms)	300.61
Sag duration (ms)	100.78
Sag initial angle (°)	354.48
Sag initial phase angle shift (°)	12.57
Sag initial phase angle shift rate (°/s)	752.44
Sag end angle (°)	22.50
Sag end phase angle shift (°)	-12.63
Sag end phase angle shift rate (°/s)	-740.58
Total harmonic distortion	0.018
rms magnitude unbalance ratio	0.415
PADD (°)	19.62

3.4. Characterization examples

This section presents the characterization results for several typical sag events. Parameters for characterizing the sag events shown in Figs. 1–3 are shown in Tables 1–3, respectively.

4. Study of equipment sensitivity during sag events

One important purpose of sag characterization is for equipment sensitivity study, i.e., how various sag parameters affect the equipment operating characteristics. Through equipment sensitivity study, one can explain why a specific load failed during a sag event, or predict how well a load will perform during a particular

Table 2
Parameters for the sag signal shown in Fig. 2

Sag parameters	Values
Minimum rms value (p.u.)	0.881
Maximum rms value (p.u.)	1.0
Average rms value (p.u.)	0.936
Final rms value (p.u.)	0.977
Peak value (p.u.)	1.415
Sag starting time (ms)	50.2
Sag recovery time (ms)	909.1
Sag end time (ms)	924.8
Sag duration (ms)	874.6
Recovery duration (ms)	15.7
Initialization angle (°)	33.43
Initial phase angle shift (°)	-1.25
Initial phase angle shift rate (°/s)	58.20
Total harmonic distortion	0.034
rms magnitude unbalance ratio	0.0064
PADD (°)	0.16

Table 3
Parameters for the sag signal shown in Fig. 3

Sag parameters	Values
Minimum rms value (p.u.)	0.0061
Maximum rms value (p.u.)	1.0
Initial sag rms value (p.u.)	0.1231
Final rms value (p.u.)	1.0
Average rms value (p.u.)	0.882
Peak value (p.u.)	1.423
Sag starting time (ms)	50.2
Sag recovery time (ms)	200.0
Sag end time (ms)	455.8
Sag duration (ms)	405.7
Recovery duration (ms)	255.8
Initialization angle (°)	332.10
Initial phase angle shift (°)	144.22
Initial phase angle shift rate (°/s)	1.72×10^4
Total harmonic distortion	0.018
Rms magnitude unbalance ratio	0.217
PADD (°)	4.38

sag event. In the following section, the overall approach for the equipment sensitivity study is described first, and then case studies for illustrating the proposed methods are presented.

4.1. Overall approach

The overall structure for evaluating the equipment behavior under voltage sag events is depicted in Fig. 6. The inputs are the voltage sag waveforms that can either be recorded in the field or be generated by specific simulation packages. The outputs are the operating characteristics of the equipment during the specified sag events. The block 'voltage sag characterization' computes the various sag parameters. The block 'sag parameter tuning' allows the user to tune or edit the sag parameters, obtained from the block 'voltage sag characterization', to certain values. The 'recorded voltage sag waveforms' provide us with a set of initial sag parameters based on which further tuning can be made. However, the recorded waveforms are optional and if they are unavailable, the user can input any desired initial sag parameters and then tune them for testing. In either case, by tuning the sag parameters such as the sag magnitude, sag duration,

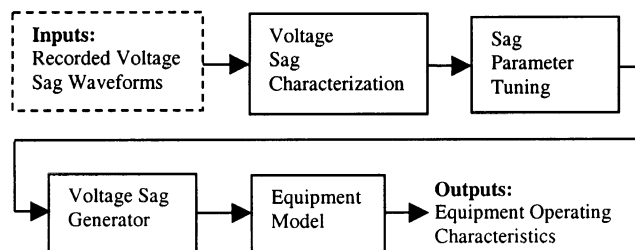


Fig. 6. The overall structure for equipment behavior evaluation.

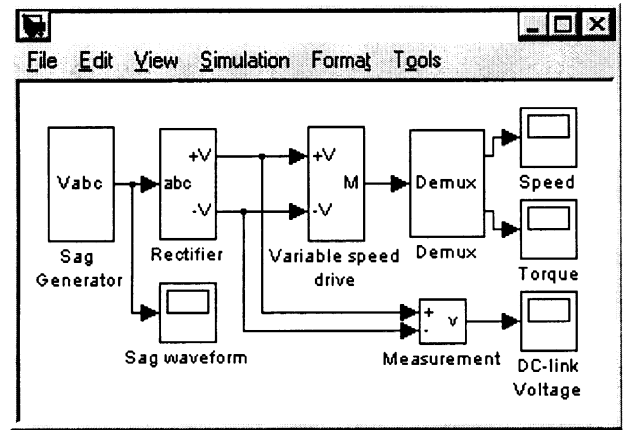


Fig. 7. The testing system diagram.

phase angle shift, etc. the software allows the user to observe and study how specific sag parameters affect the operating characteristics of the equipment under test. This is what we call the equipment sensitivity study. The block 'voltage sag generator' [8] reconstructs the voltage sag waveforms based on the tuned sag parameters. The constructed voltage waveforms serve as the voltage source for testing the equipment. The voltage sources can either be one phase or three phase depending on the equipment being evaluated. The 'equipment model' allows development of mathematical models for the equipment.

Through the sensitivity studies, the operating characteristics of the equipment during various sag events can be evaluated and responses tabulated. For example, by changing only the phase angle shift while fixing all the other sag parameters at specified values, we can obtain one table describing the equipment operating characteristics versus the phase angle shift. In the same way, the operating characteristics of the equipment versus other parameters can be obtained and archived. By comparing the parameters of a specific sag event with the saved equipment operating characteristics, automatic equipment behavior diagnosis can be realized.

4.2. Case studies

This section presents the case studies for equipment sensitivity study. The first equipment under evaluation is an induction motor fed by a current-controlled PWM (pulse width modulation) inverter. The motor is rated as 3 HP, 220 V and 60 Hz. The DC voltage is obtained by a 6-pulse diode bridge. The capacitor size at the DC side is 4.4×10^{-3} F. The inverter is built using six MOSFET blocks [9]. The speed control loop uses a proportional-integral controller to obtain the slip frequency reference that is used to control the amplitude and frequency of the three-phase controlled oscillator that produces the current references for the current

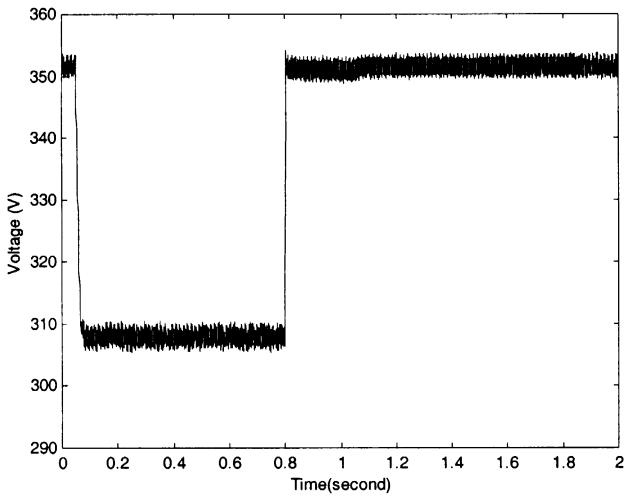


Fig. 8. The DC link voltage during a FRS event.

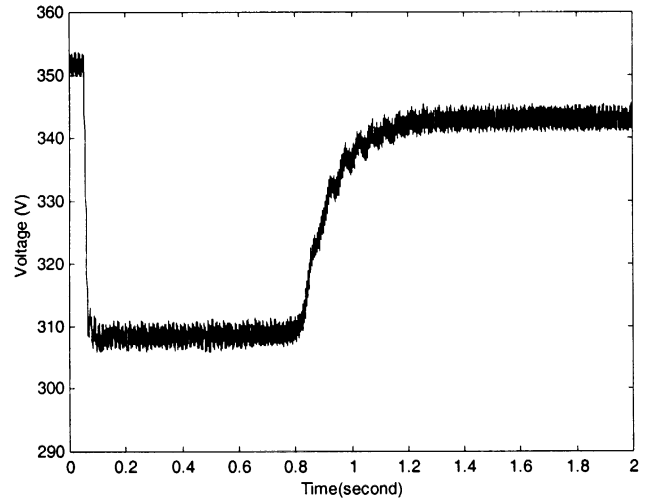


Fig. 10. The DC link voltage during a MSRS event.

controller. Fig. 7 shows the testing system diagram. In the figure, the ‘sag generator’ generates the sag waveforms with specified parameters. The ‘rectifier’ provides the DC voltage for the ‘variable speed drive (VSD)’.

Fig. 8 plots the DC link voltage during a FRS event. The rotor speed variation is drawn in Fig. 9. The voltage sag has a magnitude of 88% of the pre-sag voltage and lasts about 750 ms. It can be seen that the motor speed has a 3% drop. In contrast, Fig. 10 depicts the DC link voltage during a MSRS event that has the same magnitude as the FRS except that the MSRS has an additional recovery time of about 200 ms. The motor speed is plotted in Fig. 11. It is noted that the recovery time of the MSRS event has caused a 100 ms delay for the recovery of the motor speed compared with FRS.

Another equipment under evaluation is an asynchronous machine (ASM) directly connected to the AC bus. The ASM implements a three-phase induction machine (wound rotor or squirrel cage) modeled in the

dq rotor reference frame. It has rated values of 3 HP, 220 V, 60 Hz and 11.87 NM. Figs. 12 and 13 show the drastic variations of the electromagnetic torque and the motor speed during a FRS with a 40° of phase angle shift and no magnitude reduction. The speed of the motor has a maximum drop of 15%. This illustrates the importance of including the phase angle shift for the equipment performance evaluation.

The effects of other sag parameters on the equipment operating characteristics can be evaluated similarly. In practice, variable speed drives or ASM directly connected to the AC bus are usually protected by the relaying system that trips the AC supply when the AC voltage or DC link voltage drops below a pre-specified level. Through the equipment sensitivity study, critical values for the event parameters can be found that may be useful for the coordination between the protection system and the equipment.

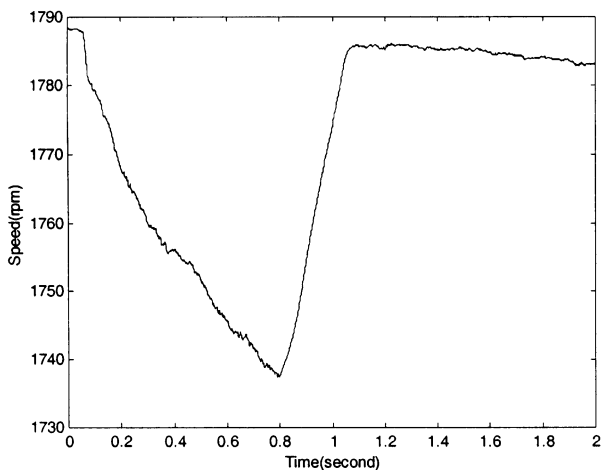


Fig. 9. The rotor speed during the FRS event.

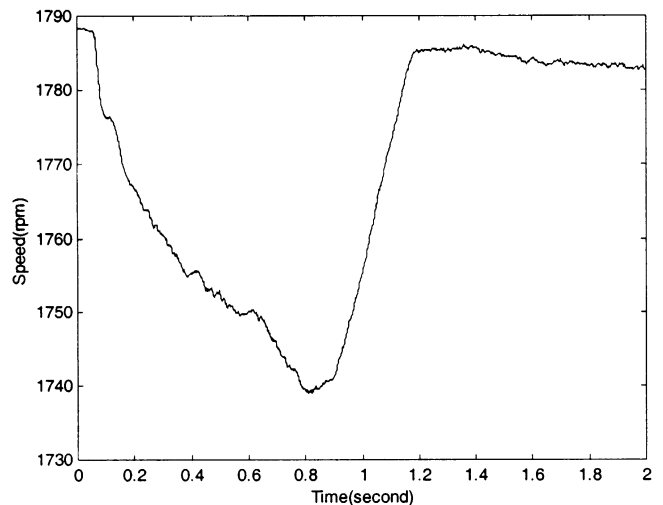


Fig. 11. The rotor speed during the MSRS event.

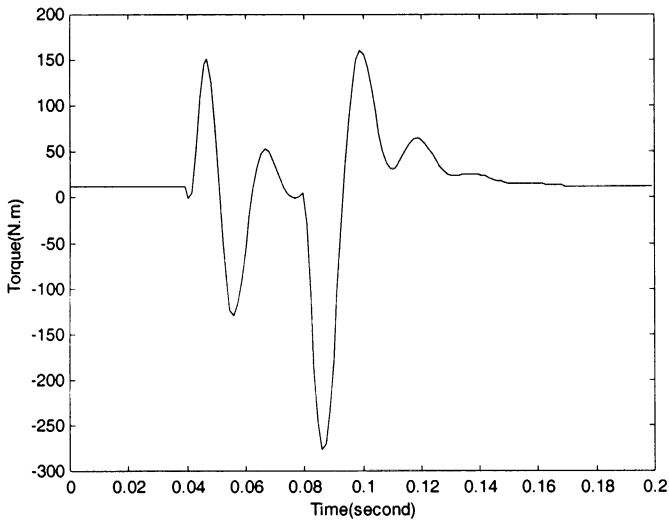


Fig. 12. The electromagnetic torque during a FRS event.

5. Conclusions

A novel fuzzy logic based sag classifier for distinguishing between the sags related to the faults, large motor starting, or to the motor re-acceleration is described in this paper. Also presented are the suggested characterization methods and parameters for the three types of sag events. The application of the characterization results for the equipment sensitivity study is illustrated. Our implementation of the algorithm in MATLAB shows that the contributions presented in the paper have promise for practical applications.

6. Nomenclature

V_{min} minimum rms value
 V_{max} maximum rms value

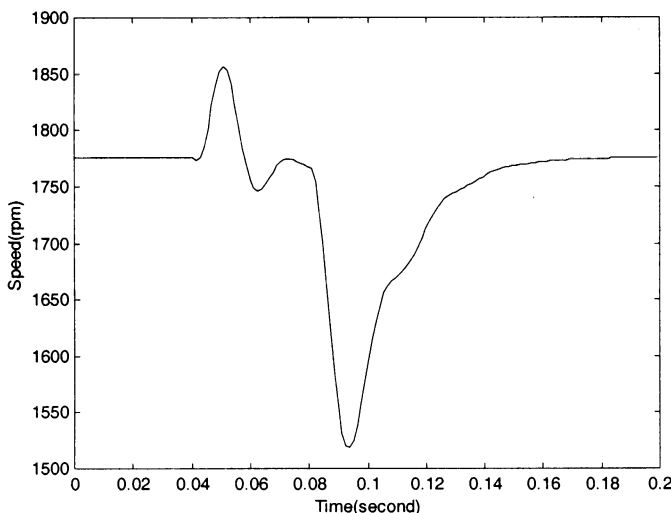


Fig. 13. The rotor speed during the FRS event.

- V_{ave} average rms value
- V_{fin} final rms value
- V_{ini} sag initial rms value
- V_p peak value
- t_s sag starting time
- t_e sag end time
- t_{sd} sag duration
- t_{rd} sag recovery duration
- α_{ini} initialization angle
- α_{pasi} initial phase angle shift
- r_{pasi} initial phase angle shift rate
- α_{end} end angle
- α_{pase} end phase angle shift
- r_{pase} end phase angle shift rate
- THD total harmonic distortion
- r_{ub} three phase rms magnitude unbalance ratio
- PADD three-phase phase angle difference deviation
- $V^n[k]$ the Discrete Fourier Transform (DFT) of the signal in the n th data window
- $V^s[k]$ the Discrete Fourier Transform (DFT) of the signal in the first window after the sag event
- $V^{sa}[k], V^{sb}[k]$ and $V^{sc}[k]$ $V^s[k]$ applied to phase a, b and c signals respectively
- $V^e[k]$ the Discrete Fourier Transform (DFT) of the signal in the first window after the sag recovery
- i_s sag starting point
- i_e sag end point
- i_p instantaneous voltage peak point
- i_{min} minimum rms voltage cycle index
- i_{zi} the last positive zero crossing point of the pre-sag waveform
- i_{ze} the last positive zero crossing point of the during-sag waveform
- f_0 the fundamental frequency of the system
- f_s the sampling frequency of the signal
- $v[i]$ the sampled signal of phase A, B, or C, $i = 0, 1, \dots, L-1$
- L the length of the signal
- N the number of samples in one data window (one cycle)
- j the imaginary unit
- $WC_1[k]$ the first scale wavelet detail coefficients, $k = 1, 2, \dots, L_{WC_1}$
- L_{WC_1} the length of $WC_1[k]$
- ε a pre-defined constant, selected as 0.05 here
- P_{ab} the angle difference between phase A and phase B voltages
- P_{bc} the angle difference between phase B and phase C voltages

P_{ca}	the angle difference between phase C and phase A voltages
P_{pad}	the array composed of P_{ab} , P_{bc} , and P_{ca}
V_{rms}^t	an array composed of $V_{rms}[n]$, $n = 1, 2, \dots, L_{rms}^t$
L_{rms}^t	length of V_{rms}^t defined as round (L/N)
$V_{rms}[n]$	rms value of the signal in the n th data window (cycle)
V_{rmss}	rms value of the signal in the data window immediately after the sag occurrence
$V_{rmssabc}$	an array composed of V_{rmssa} , V_{rmssb} , and V_{rmssc}
V_{rmssa} , V_{rmssb} , V_{rmssc}	V_{rmss} applied to phase a, b and c signals respectively
V_{rms}^{td}	an array composed of $V_{rms}[n]$, $n = i_{min}, \dots, L_{rms}^t$
i_{re}	sag recovery index in cycle
i_{ec}	sag end index in cycle

Acknowledgements

The developments reported in this paper are funded by the Texas Higher Education Coordinating Board Advanced Technology Program. The co-funding is pro-

vided by TXU Electric and Gas and Reliant Energy HL&P.

References

- [1] IEEE Project 1346 Working Group, Electric Power System Compatibility with Industrial Process Equipment, part 1: Voltage Sags, IEEE Industrial and Commercial Power Systems Technical Conference, Irvine, CA, USA, May 1–5, 1994, pp. 261–266.
- [2] Mladen Kezunovic and Yuan Liao, Automated voltage sag characterization and equipment behavior analysis, International Conference on Power Quality, Electrical Power Systems World'99, Chicago, November 1999.
- [3] IEEE P1159.2, Task Force on Characterization of a Power Quality Event Given an Adequately Sampled Set of Digital Data Points, web site: <http://grouper.ieee.org/groups/1159/2/keypts.html>.
- [4] E.R. Collins and A. Mansoor, Effects of voltage sags on AC motor drives, Proceedings of the 1997 Textile, Fiber, and Film Industry Technical Conference, 97CH36100, May 6–8, 1997, pp. 1–7.
- [5] J.C. Das, Effects of momentary voltage dips on the operation of induction and synchronous motors, IEEE Trans. Ind. Appl. 26 (4) (1990) 711–718.
- [6] Math H.J. Bollen, The influence of motor re-acceleration on voltage sags, IEEE Trans. Ind. Appl. 31(4) (1995) 667–674.
- [7] John Yen, Reza Langari, Fuzzy Logic: Intelligence, Control, and Information, Prentice Hall, Englewood Cliffs, NJ, 1999, pp. 3–18, 63–68.
- [8] Mladen Kezunovic, Yuan Liao, A novel method for equipment sensitivity study during power quality events, IEEE PES Winter Meeting, 2000, Singapore.
- [9] MathWorks, Inc., MATLAB Manuals, May 1997.